

A new extant family of primitive moths from Kangaroo Island, Australia, and its significance for understanding early Lepidoptera evolution

NIELS P. KRISTENSEN^{1*}, DOUGLAS J. HILTON²,
AXEL KALLIES², LIZ MILLA², JADRANKA ROTA³,
NIKLAS WAHLBERG³, STEPHEN A. WILCOX⁴,
RICHARD V. GLATZ^{5,6,7}, DAVID A. YOUNG⁵, GLENN COCKING⁸,
TED EDWARDS⁸, GEORGE W. GIBBS⁹ and MIKE HALSEY¹⁰

¹Natural History Museum of Denmark (Zoology), University of Copenhagen, Copenhagen Ø, Denmark, ²Department of Zoology, University of Melbourne, Parkville, Australia, ³Laboratory of Genetics/Zoological Museum, Department of Biology, University of Turku, Turku, Finland, ⁴The Australian Genome Research Facility, Parkville, Australia, ⁵D'Estrees Entomology & Science Services, Kingscote, Australia, ⁶School of Agriculture, Food and Wine, The University of Adelaide, Urrbrae, Australia, ⁷South Australian Museum, Terrestrial Invertebrates, Adelaide, Australia, ⁸Australian National Insect Collection, CSIRO, Canberra, Australia, ⁹School of Biological Sciences, Victoria University, Wellington, New Zealand and ¹⁰Murray-Darling Freshwater Research Centre, La Trobe University, Wodonga, Australia

Abstract. We report the first discovery since the 1970s of a new extant family (Aenigmatineidae **fam.n.**) of homoneurous moths, based on the small *Aenigmatinea glatzella* **sp.n.** from Kangaroo Island off southern Australia. It exhibits a combination of extraordinary anatomical characters, and, unlike most homoneurous moths, its larva is a conifer-feeder (stem mining in *Callitris*, Cupressaceae). While the adult's mouthparts are strongly regressed, evidence from other morphological characters and from a Bayesian analysis of 25 genetic loci convincingly places the taxon among Glossata ('tongue moths'). An unexpected tongue moth clade including Acanthopteroctetidae and Neopseustidae, suggested with low support in recent molecular analyses, remarkably becomes strongly supported when *Aenigmatinea* is included in the molecular analysis; the new taxon becomes subordinated in that clade (as sister group to Neopseustidae) and the clade itself appears as the sister group of all Heteroneura, representing the vast majority of all Lepidoptera. Including *Aenigmatinea* into the analysis thereby strengthens the surprising indication of non-monophyly of Myoglossata, and the new phylogeny requires an additional number of *ad hoc* assumptions of convergence/character reversals in early Lepidoptera evolution.

This published work has been registered in ZooBank, <http://zoobank.org/urn:lsid:zoobank.org:pub:44393B52-1889-431A-AB08-6BBCF8F946B8>.

Introduction

The great majority (>99%) of the extant members of the 'megadiverse' order Lepidoptera (moths and butterflies) pertain to the monophylum Heteroneura, characterized in its ground

plan by the specialized condition of having the hindwings coupled to the forewings in flight, and a (surely correlated) marked difference in their venation relative to that of the forewings, particularly noticeable in the reduced number of anterior longitudinal vein branches. The remaining small fraction, the 'homoneurous grade', comprises the most primitive families in the order, i.e. the families that originated first during lepidopteran evolution. This homoneurous grade comprises the non-glossatan families ('jaw moths'), of which the constituent Micropterigidae, Agathiphagidae and Heterobathmiidae have

Correspondence: Niklas Wahlberg, Department of Biology, University of Turku, 20014 Turku, Finland. E-mail: niklas.wahlberg@utu.fi

*Deceased December 6th, 2014.

retained functional mandibles throughout adult life and are primarily devoid of a coilable 'tongue', as well as an assemblage of families in which the adults' mandibles are non-functional in the post-pharate phase, and a coilable proboscis for uptake of fluids is present (if not secondarily reduced). These specializations of the assemblage are shared with the Heteroneura, and, together with the latter, it forms the clade Glossata ('tongue moths').

In what has been a near-consensus reconstruction of the lepidopteran family tree, most of the homoneurous families arose in a comb-like fashion, instructively demonstrating 'additive typogenesis', i.e. the sequential acquisition of specializations characterizing a large and well circumscribed group (*in casu* Heteroneura) (Hennig, 1966; Ax, 2000; Grimaldi & Engel, 2005; Kristensen *et al.*, 2007). Recent molecular analyses have challenged this simple picture of early lepidopteran evolution (Mutanen *et al.*, 2010; Regier *et al.*, 2013), thereby implying unexpected anatomical homoplasy (convergences and/or character reversals). However, some of the most striking classificatory changes were only weakly to moderately supported and the picture has remained incomplete due to the scarcity of known surviving representatives of these early-evolved lineages. No new extant homoneurous moth families have come to light since the 1970s.

We report here the discovery of a new family of homoneurous moths, based on the small *Aenigmatinea glatzella* **gen. et sp.n.** from Kangaroo Island off southern Australia. We outline its life history and describe its principal structural characteristics. Finally, we examine how the inclusion of *Aenigmatinea* in molecular analyses affects the resulting tree, and we discuss how the ensuing placement of *Aenigmatinea* affects current understanding of early lepidopteran evolution through the requirement for additional *ad hoc* assumptions of morphological homoplasy.

Material and methods

Field work and life-history observations

The first two adult females were captured on 5 and 19 October 2009. Other specimens were collected during October in 2012 and 2013. The capture of adults was generally by the use of fine-mesh nets, sweeping over and around the host trees, *Callitris gracilis* R. T. Baker (Cupressaceae). In one case, a malaise trap yielded a female adult. Adult moths that were selected for pinning were killed using volatile ethyl acetate.

Adult females were observed running over and probing with their ovipositor into growing tips of foliage of the host plants. Some of these tips were removed from the plant and subsequently dissected using fine-pointed forceps under a dissecting microscope to confirm the presence of the egg. Several plants where significant female activity was seen were tagged for future observation. *Callitris* cones (closed and dehiscent) were collected to store for potential emergence of adults; no *Aenigmatinea* were found in these cones.

Between January and March 2013, foliage and small (*c.* ≤ 2 cm diameter) branches were carefully examined for

larvae or traces of larval activity, and split or stripped of bark. Stripping of the bark revealed the characteristic *Aenigmatinea* larval chambers, which yielded larvae of varying sizes, pupae and several dead adults. Some chambers were empty. Branches containing these chambers were examined for other evidence of larval activity (e.g. tunnels) but none was found, except for several cases of small emergence holes in the bark, and feeding scars on the bark's underside, both at the site of the larval chamber.

Morphological examinations

The morphological observations were primarily based on material not included in the paratype series, but with the same locality/dates (see later): five males and nine females preserved dry or in Pampel's fluid. Anatomical preparations (critical-point dried mounts, slide mounts, serial sections, scanning electron microscopy stubs) have been deposited in the Natural History Museum of Denmark, University of Copenhagen.

Observations and dissecting-microscope photographs were made on material fixed in untreated alcohol or Pampel's fluid (Upton & Mantle, 2010) (Fig. 4k, n). Most dried adult material and the head of one Pampel-fixed larva were examined after standard KOH clearing. Preparations were photographed in incident light while immersed in glycerol (Fig. 2a) or by bright-field microscopy as euparal-embedded slide mounts, either unstained (Figs 2c, 4a, g) or after staining in chlorazol black (Fig. 4c, d, f, l, m; Figure S1a, b). KOH-treated and -stained male postabdomens of a few specimens were embedded in paraplast, part of the body wall of one side sectioned away on a microtome, and euparal-embedded whole-mount preparations were subsequently made after dissolution of the block in xylene (Fig. 4d, f).

Some material fixed in Pampel's fluid was critical point-dried after dehydration in an ascending ethanol series and subsequently examined/photographed in a dissecting microscope (Figs 2b, 3a, c). Scanning electron microscopy (Jeol JSM-6335F) was made of specimens that had been air-dried (Figs 2d, 3d, e) or Pampel-fixed and critical point-dried (Figs 2e, h, i, 3j; Figure S1e). Semi-thin serial sections were made of Pampel-fixed material embedded in historesin, sectioned at 1 μ m thickness, and stained with a mixture of toluidine blue, borax (each four parts of 1% aqueous solution) and pyronin G (one part of 1% aqueous solution) (Figs 2f, g, 3b, j, 4e, h, i).

Molecular sequencing and analysis

Two females were used for DNA extraction and their remnants preserved in ethanol. The molecular dataset includes three Trichoptera outgroup taxa and 59 lepidopteran ingroup taxa with sequences from 25 genetic loci. Sixteen of these loci were sequenced for *A. glatzella*, while sequences for all other taxa come from published studies (Mutanen *et al.*, 2010; Regier *et al.*, 2013). All taxa, loci, and their GenBank accession numbers are listed in Table S1, and the numbers of base pairs for each locus are listed in Table S2.

Sequence data for *A. glatzella* were obtained by PCR amplification of carbamoylphosphate synthetase (CAD) and wingless using primers from Wahlberg & Wheat (2008) and by sequencing of transcriptomes for the other 14 loci. For the transcriptome sequencing, two adult female moth specimens were pooled and 12 larval specimens were pooled to generate total RNA. The RNA was prepared according to the Macherey–Nagel NucleoSpin® RNA XS protocol. The integrity and quantity of the individual pooled RNA samples were assessed on the Agilent Tapestation using the R6K tape and reagents. An input of 100 ng of total RNA from the adult pool and the larval pool were prepared and indexed separately for Illumina sequencing using the RNA TruSeq RNA sample Prep Kit (Illumina, San Diego, CA, U.S.A.) as per manufacturer's instruction. Each library was quantified using the Agilent Tapestation and the Qubit™ RNA assay kit for Qubit 2.0 Fluorometer (Life Technologies, Carlsbad, CA, U.S.A.). The indexed libraries were pooled and diluted to 12 pM for single-end sequencing on a MiSeq instrument using the v3 300 cycle kit (Illumina) as per the manufacturer's instructions.

The Illumina reads were prepared for assembly by trimming the 3' end by 50 bases (minimum remaining length of 75 bases) then quality trimming using the Burrows–Wheeler trimming algorithm (Li & Durbin, 2009) with a cutoff Phred score of 20. Trimmed reads from adults and larvae were combined into a single file for assembly and corrected for substitution errors using MUSKET version 1.1 (Liu *et al.*, 2013). We used two assembly programs, TRINITY version r20131110 (Grabherr *et al.*, 2011) and VELVET version 1.2.10 (Zerbino & Birney, 2008) together with OASES version 0.2.8 (Schulz *et al.*, 2012), to create de novo transcriptome assemblies from the combined data. All assembled transcripts were searched using BLASTN against a nucleotide database created from published gene sequences (Wahlberg & Wheat, 2008; Rota-Stabelli *et al.*, 2013), and downloaded from GenBank. The transcript with the best alignment to each gene (based on an E-value threshold of 10^{-5} and a minimum alignment length of 250 bases) was selected and used as a new reference. The trimmed RNA reads were mapped against the new reference using BOWTIE 2.0.5 (Langmead & Salzberg, 2012). Coverage for each transcript was visually checked using IGV version 2.2.0 (Thorvaldsdottir *et al.*, 2013). Heterozygous sites appearing in adult or larval sequences were manually updated with the degenerate code and transcripts were trimmed to areas of uniform coverage. Cytochrome c oxidase subunit I (COI), elongation factor 1 alpha (EF-1 α), glyceraldehyde-3-phosphate dehydrogenase (GAPDH) and dopa decarboxylase (DDC) sequences were also validated against data previously obtained by Sanger sequencing.

All 25 genetic loci included in this dataset are protein-coding genes. One is mitochondrial (COI), and the others are nuclear. The full dataset has 19 512 base pairs (see Table S2 for details). The data were managed and datasets were created using the web application VoSeq (Peña & Malm, 2012). We created eight different datasets, each with the same taxon composition but differing in the type and amount of data excluded and the partitioning strategy applied (Table S3). Using the program TIGER (Cummins & McInerney, 2011), all of the sites in the

alignment were sorted into 80 bins based on their relative evolutionary rate, with invariable sites being sorted into bin 1, and the fastest-evolving sites into bin 80. The bins were then combined into partitions as described by Rota & Wahlberg (2012), resulting in eight partitions (partition 1 contained the slowest-evolving sites and partition 8 the fastest-evolving sites). In some of the analyses, as described later, the fastest partitions were excluded. The final datasets were as follows: (1) full (all sites included); (2) full_ex8 (partition 8 excluded); (3) full_ex78 (partitions 7 and 8 excluded); (4) full_ex678 (partitions 6, 7, and 8 excluded); (5) coi_no3rd (third codon positions of COI excluded); (6) coi_no3rd_ex8 (partition 8 excluded); (7) coi_no3rd_ex78 (partitions 7 and 8 excluded); and (8) no3rd (third codon positions of all genes excluded) (Table S3).

All eight datasets with their different partitioning strategies were analyzed with MRBAYES v3.2 on the CIPRES (Miller *et al.*, 2010) server, and the datasets full and no3rd were additionally analysed with RAXML (Stamatakis *et al.*, 2008) as unpartitioned. In Bayesian analyses the priors were set to the default values, with the exception of the branch length prior [brlensp = unconstrained:Exp (100.0)] to avoid the potential problems of trees that are too long (Brown *et al.*, 2010; Marshall, 2010). We used the mixed model for nucleotide substitutions and modelled the among-site rate variation with the alpha parameter of the gamma distribution, without including the proportion of invariable sites to avoid confounding effects of these two parameters on each other (Ren *et al.*, 2005). Analyses were run for 20 million generations, with one cold and three heated chains, sampling trees every 2000 generations, and with a burn-in of 25%. Convergence was checked in TRACER v.1.5 (Rambaut & Drummond, 2007) and by examination of the potential scale reduction factors and split frequencies, both reported by MRBAYES. RAXML (Stamatakis *et al.*, 2008) analyses were conducted using the RAXML BlackBox applying the gamma model of rate heterogeneity and using the maximum likelihood search, with 100 bootstraps.

Results

Taxonomy

Order LEPIDOPTERA, homoneurous grade

Aenigmatineidae Kristensen & Edwards, fam.n.

<http://zoobank.org/urn:lsid:zoobank.org:act:AF88BFAD-76C5-4B25-9961-2481194A8071>

Aenigmatinea Kristensen & Edwards, gen.n.

<http://zoobank.org/urn:lsid:zoobank.org:act:47CC5617-BF1E-4E64-8531-9EDB493CCB69>

Aenigmatinea glatzella Kristensen & Edwards sp.n. (type species)

<http://zoobank.org/urn:lsid:zoobank.org:act:B40F4FD5-3650-491E-A6BC-5FA966079AE0>

Diagnosis. Adult moths (Fig. 1a) small, forewing length \approx 4 mm, immediately recognizable by unique combined

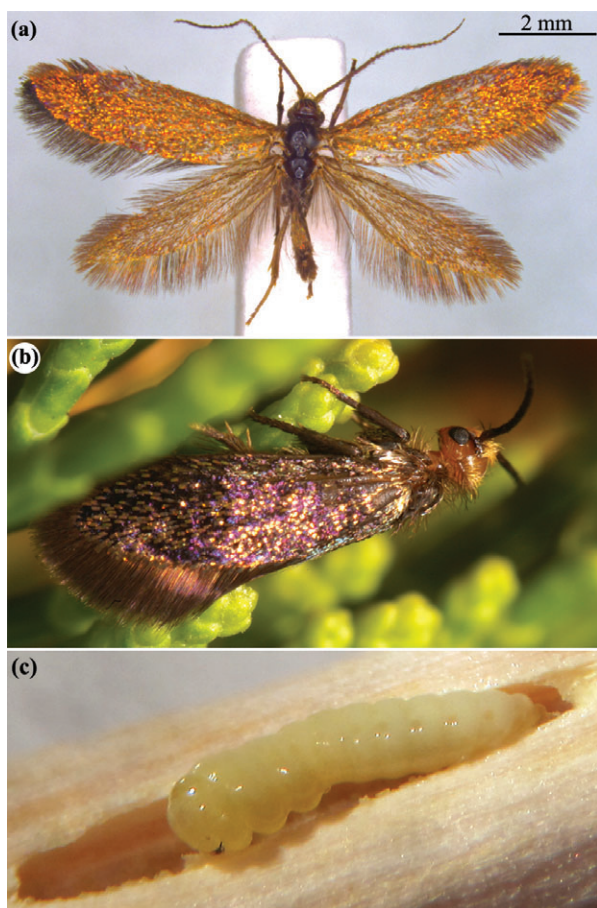


Fig. 1. *Aenigmatinea glatzella*. (a) Male holotype; (b) female in typical upside-down posture on young foliage of host (*Callitris gracilis*); (c) larva partly removed from terminal cell inside *Callitris* stem.

presence in the forewing (Fig. 3f) of a prominent jugal lobe, an only two-branched radial sector and a single-branched medial vein.

Aenigmatinea Kristensen & Edwards gen.n.

Type species. *Aenigmatinea glatzella* Kristensen & Edwards **sp.n.** by monotypy.

Anatomical characters as for family, see the section on 'Principal morphological characteristics of *Aenigmatinea*'.

Etymology. Gender feminine, referring to enigmatic character combination; the Linnean *Tinea* comprised the many small moths, including the small homoneurans, whose wing posture in repose made them appear cylindrical ('*Alis convolutis fere in cylindrum ...*') (Linné, 1767).

Aenigmatinea glatzella Kristensen & Edwards **sp.n.**

Holotype data. ♂, AUSTRALIA, South Australia, Kangaroo Island, on private property, 1 km N of Willson River mouth, Mouth Flat, 35°51'S/137°56'E, 5. x. 2012 (South Australian Museum, Adelaide). **Paratypes:** 26♂♂, 39♀♀, October 5 and

19, 2009 and October 3–13, 2012, locality data as holotype (Australian National Insect Collection, CSIRO, Canberra; South Australian Museum, Adelaide; Natural History Museum of Denmark, University of Copenhagen; National Museum of Natural History, Smithsonian Institution, Washington, DC; Natural History Museum, London; Museum National d'Histoire Naturelle, Paris; Zoological Museum of the Humboldt University, Berlin, Germany; private collections of R. Glatz, A. Kallies, M. Halsey).

Etymology. Adjective, gender feminine, honoring the moth's discoverer R. V. Glatz; the name also alludes to the unusual dearth of head scales, *Glatze* being German for a bald head.

Description. Anatomical characters as for family/genus, see the section on 'Principal morphological characteristics of *Aenigmatinea*'. Head capsule shining, in male blackish (Fig. 1a), in female largely bright orange-yellowish (Fig. 1b), lower part (below interocellar sulcus) light brownish. Antennal scales black, on scape long and piliform, on flagellum lamellar. Cranial piliform scales mostly light yellowish-brownish, posterior group on posterolateral beds black. Forewing length/width ratio ≈ 2.8 . Forewing scale vestiture iridescent, changing markedly with incidence of light, appearing brownish-purplish with \pm extensive suffusion of gold, but without any golden band-and-spot pattern. Hindwing greyish-brownish with modest golden iridescence. Marginal hair-scales ('fringes') uniformly greyish brown, with weak purple sheen.

Bionomics

Adult *Aenigmatinea* are diurnal and apparently short-lived. They have been observed only between late September and October, around *Callitris gracilis* on which females oviposit. Males were seen flying actively over *Callitris* in the morning. Uptake of fluids (probably by immersing the lower/anterior head portion in water drops) has not been observed, but is inferred from the robust development of the sucking pump with its strong musculature and prominent sitophore, which is an adult structure, not one retained from the larva. The female's long, extensible oviscapt is used for inserting the egg below a bract near the growing tip (Figure S1e), at the junction between the main stem and the developing branch. Larval feeding scars are visible on the underside of the bark and correspond to the larval chambers (Fig. 1c), indicating that larvae remain here and feed on the phloem and/or callus tissue on the interior surface of the adjacent bark. No indications of tunnels between branch apices and definitive cells (often located 30 cm or more from the affected branch apices) have been found. The young larva is likely to make its chamber in the stem tissue close to the oviposition site, and depending on whether chamber formation has taken place around the time of, or sometime after, the beginning of elongation of the main branch and side branch (formed at the base of the enclosing bract), the chamber may be located close to, or distad to, the branch junction. Small and large larvae have been observed at the same time, and hence larval development probably spans more than one season.

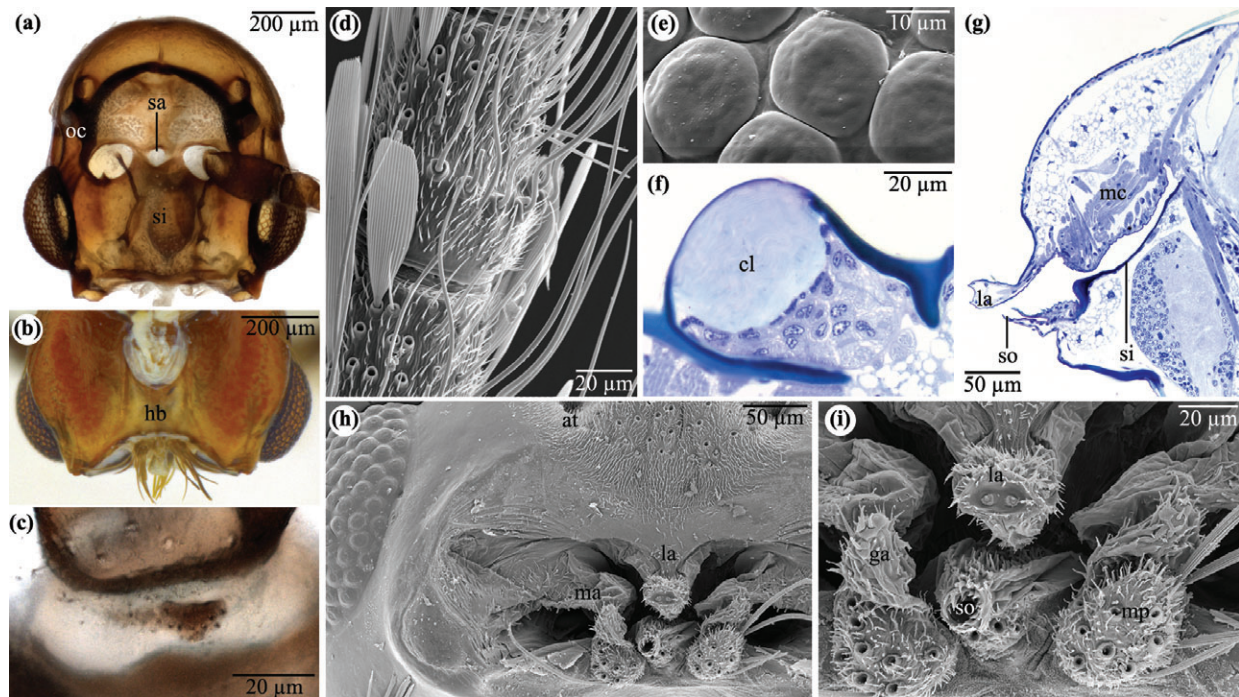


Fig. 2. *Aenigmatinea glatzella* head structures. (a) Female head anterior view, right antenna removed; (b) male head, posterior view of lower part; (c) membrane between antennal scapus (below) and pedicellus, with generalized type (near-triangular, microtrichiated) intercalary sclerite; (d) male flagellomeres, with dorsal scale vestiture and S-bent bases of long sensilla trichodea; (e) compound eye, ommatidia surface; (f) ocellus, transverse section; (g) lower part of head, median section; (h, i) ventral part of head showing vestigial mouthparts. at, anterior tentorial pit; la, thickened cuticular lens; ga, galea vestige; hb, hypostomal bridge; la, labrum; ma, soft-walled mandible; mc, muscular coat of sucking pump; mp, maxillary palp; oc, ocellus; sa, sinus attachment site; si, sitophore; so, salivary opening on apex of prelabio-hypopharyngeal cone.

Conservation issues

The Kangaroo Island fauna is poorly known, and the suggestion (Davies *et al.*, 2002) of low species-level endemism may well prove incorrect, but with 19 species of *Callitris* being broadly distributed on mainland Australia and New Caledonia (Pye *et al.*, 2003), the discovery of additional *Aenigmatinea* populations or species seems possible. *Callitris gracilis*, with two recognized subspecies, is quite widely distributed across south-eastern Australia in South Australia, Victoria and New South Wales, with outlying records in the east of Western Australia (ABRS, 1998). It is noteworthy, however, that the known range of *A. glatzella* on the island is restricted, and targeted searches for the species where the host occurs in other nearby (but isolated) similar sites have so far been unsuccessful. Action for appropriate conservation and management of the known habitat of this unique insect is thus a matter of considerable urgency.

Principal morphological characteristics of *Aenigmatinea*

This account emphasizes autapomorphies and phylogenetically potentially significant traits; several additional descriptive details, and some figures, are given in Appendix S1 and Figure S1, respectively.

(i) Adults. Head-capsule with unique hyaline spot between antennal bases (Fig. 2a) demarcating attachment area of anterior blood sinus (aorta continuation in front of brain). Capsule posteroventrally closed by hypostomal bridge (Fig. 2b), the length/strength of which is unparalleled in Lepidoptera; it probably includes a territory pertaining to the otherwise uniquely regressed labium. Antennae with intercalary sclerite in scapopedicellar membrane triangular, strongly melanized and microtrichiated (Fig. 2c). Flagellomeres near-cylindrical, dorsally scaled, in male with slightly raised proximal zone bearing a whorl of very long, basally markedly S-bent sensilla trichodea (Fig. 2d); there is no longitudinal alignment of hairs/scales. Ommatidia of compound eyes partly separated by narrow strips of melanized cuticle, their surface smooth (Fig. 2e). Ocellar cuticle forming thickened lenses (Fig. 2f), a condition characterizing advanced Lepidoptera and unique among the few homoneurous moths that retain ocelli. Externally visible mouthparts (Fig. 2h, i) more strongly reduced than in any other non-hepialoid homoneurous moths. Labrum small, unsclerotized and very narrow, widening towards the apex. Mandibles are sizeable lobes, but obviously incapable of biting, being devoid of teeth and soft-walled, except for melanized basal margins adjacent to invaginations of apodemes for the strongly developed ad- and abductor muscles, whose origins cover a large portion of the cranial surface; in the pharate stage they can move the pupal mandibles into which they

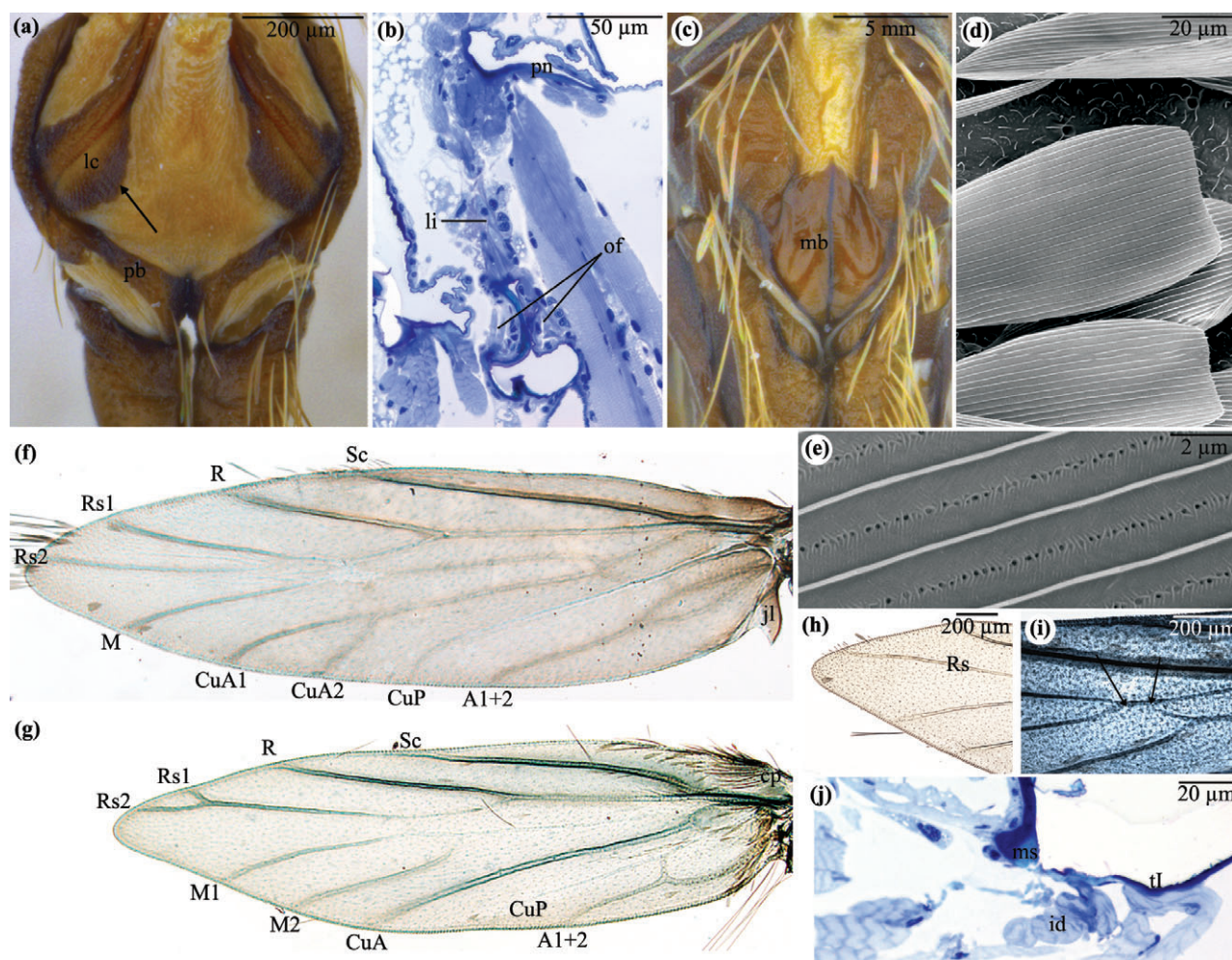


Fig. 3. *Aenigmatinea glatzella*, thoracic/thoracic-abdominal structures. (a) Prothorax, anterior view; (b) first thoracic spiracle (anterior to right), tangential section; (c) mesothoracic pleurosternum, anterior view; (d, e) surface scaled on forewing upper side, with perforations (e) in cover scale; (f, g) descaled forewing (f) and hindwing (g); (h) hindwing, specimen with unbranched radial sector (Rs); (i) hindwing, subapical (apical to left) region in specimen with continuation of the media (M) stem anastomosing with the Rs stem (arrows); (j) dorsal thoraco-abdominal transition, sagittal section. A, anal veins (in forewing with typical amphiesmenopteran basal Y-configuration), C, costa; cp, cluster of piliform scales; CuA, anterior cubitus; CuP, posterior cubitus; id, indirect (hind) wing depressor; jl, jugal lobe; lc, laterocervical sclerite with un-produced postero-median corner (arrow); li, opener ligament; mb, mesobasisternum; ms, metascutellar margin; of, occlusor fibres; pb, precoxal bridge; pn, pronotum; R, radius; Sc, subcosta; tl, tergum I.

fit. Maxillae, minute bilobed protuberances, situated behind mandibles and on each side of median prelabio-hypopharyngeal process. The outer lobe is a palp vestige; the inner is the galea, largely unsclerotized and with close-set sensilla on the apex. Prelabio-hypopharyngeal process is an unsclerotized median conical lobe, the apex bearing a prominent orifice leading into a very short, vestigial salivarium pocket (Fig. 2g); a few slender fibres of the dorsal (hypopharyngeal) salivarium dilator muscle are retained, but no glandular tissue associated with the salivarium pocket has been identified. The lobe portion (which must be labial) behind/below this orifice probably represents a ligula and is the only identifiable element in the uniquely reduced labium; palps being completely absent. Sitophore sclerotization (Fig. 2a, g) remarkably large, thick and strongly melanized, without obvious gustatory sensilla, markedly tapering anteriorly,

inner/posterior end abruptly truncated. Dorsal/anterior sucking pump musculature strong. Unlike in pre-glossatans there is no free tritocerebral commissure below the precerebral food tract.

Laterocervical sclerites slender, stiffened for their entire length by prominent linear thickening; posteromedian margin truncated, not in any way produced towards mid-line (Fig. 3a). Precoxal pleurosternal bridge (Fig. 3a) very strongly developed. First thoracic spiracle (Fig. 3b) of 'Coelolepida type' (Davis, 1975) in which an atrial sclerotization is produced into a simple apodemal 'lever'; opening is performed by an elastic ligament from the pronotum to the lever apex, while occlusion is due to contraction of muscle fibres between lever apex and the adjacent atrial wall on both sides of the lever. Mesobasisternum strengthened by median ridge and anteriorly moderately convex,

but with at most a tiny median process (Fig. 3c). Scale covering on upper forewing surface \pm distinctly two-layered, scales near-triangular, apical margin almost straight, ground scales somewhat smaller than cover scales. Cover scales on forewing surface (Fig. 3d, e) with aligned small pores in middle of inter-ridge areas, 'flutes' distinctly developed around pores, becoming obsolete towards ridges. Ground scales may be pore-less. Forewing (Fig. 3f) with jugal lobe strongly developed. Hindwing (Fig. 3g) at base (before very indistinct humeral vein) without 'frenulum bristles' on costa, but with a cluster of long, pointed-hair-like piliform scales extending backwards from costa, a condition so far unrecorded from homoneurous moths. Wing venation simplified to a degree also unparalleled in homoneurous moths. Forewing radial sector (Rs) represented by a single pre-apical fork. Media (M) vein single-branched; the nerve in its distal part is received from Rs via a cross-vein in the subapical area, where all veins can be extremely faint, but the identification of this distal vein as an M branch is not questioned here. In the hindwing the single Rs branch may have a small subapical fork or may be unbranched (Fig. 3g, h). The post-apical venation is particularly unique and intriguing. Here only three veins reach the wing margin anterior to posterior cubitus (CuP), and the identity of these veins (subject to some individual variation) is in some cases difficult to ascertain. The most anterior is interpreted as the counterpart of the forewing M, as it may appear as a continuation of the M stem, being for its whole length clearly separate from Rs (Fig. 3g); like the forewing M it receives a nerve from Rs. However, in some cases the M stem continuation approaches, and almost or completely anastomoses with the pre-apical Rs (as in forewing it may be quite indistinct in the area in question); the distinct distal part of the first post-apical vein in this situation may superficially appear as an Rs branch (Fig. 3i). The following vein has a faint (but in some preparations distinct, particularly after intense staining; Fig. 3i) basal connection to the M stem and it is considered to be most likely another M branch. In this case, then, it has no counterpart in the forewing, which would be a most exceptional condition in a homoneurous moth. But the *a priori* more likely alternative of it being the usually present anterior cubitus branch 1 (CuA1; and its basal connection to M thus a cross-vein) is not supported by the actual configuration: no trace of a connection to the following vein has been observed. The third is undoubtedly a CuA branch (1 or 2).

Anterior margin of tergum I flat, hence indirect hindwing depressors insert on a near-horizontal surface (Fig. 3j). Anterior tergal sclerotization extending far backwards, covering almost entire dorsum I (Fig. 4a), a condition without counterparts in other homoneurous moths, where only the margins are sclerotized. Sternum V gland with opening bearing papilla unlike counterparts in other Lepidoptera, unmelanized and with near-circular flattened-depressed surface; only few and low tubercles present behind opening slit (Fig. 4b). Male genital apparatus particularly noteworthy for presence of a 'transtilla' (Fig. 4c, d, e), a medially elongate sclerotization located above the phallus and anteroventrally extended into a pair of arms which enclose the phallocrypt and eventually are continued into

paired dome-shaped sclerotizations formed by fused inner valve bases and posterior segment IX sclerotization; the posterior transtilla apex is cleft, forming a pair of upward-bent hooks. Also exceptional is the overall simple sclerotized phallic tube, which, a short distance behind the anterior end, has a distinct unsclerotized and flexible zone (Fig. 4f), seemingly without counterpart in other homoneurous Glossata with a sclerotized phallus. Female postabdomen an '*Eriocrania*-type' oviscapit (Davis, 1975) with segment VIII forming a completely sclerotized, lopsided cone (Fig. 4g; Figure S1e) with long/strong 'anterior apophyses' extending forwards from front margin. Dorsomedian cone portion extending backwards markedly beyond the posterolateral and -ventral margins, forming blunt, markedly downward-curving and excessively melanized 'dorso-terminal lobe'. Posterior-most part of abdomen formed by a long flattened-cylindrical unsclerotized collar with a demarcated transverse fold, and a terminal unit comprising two lateral sclerotized rods which converge strongly towards the apex where they are united by a dorsal sclerotization and are anteriorly continued into long apodemal 'posterior apophyses'. Their posterior/terminal external portions (Fig. 4j) are devoid of true 'saw teeth', but the flat, bluntly rounded body wall apex bears a few minute, delicate and downward-bent hooks; this is consistent with the eggs being inserted between free parts of the plant, rather than bored into plant tissue. Colleterial gland wall composed of 'type 1' gland cells (Fig. 4h). Ovarioles may extend forwards to the meso-prothoracic boundary, without oocyte/nurse cell clusters: even the most anterior identifiable oocytes are yolk-filled and chorionated (Fig. 4i); to our knowledge this is a previously unrecorded condition in adult Lepidoptera.

(ii) Larva. All trunk segments devoid of sclerotizations/pigmentation; legs and prolegs absent. Head capsule (Fig. 4k, l, m) thin and largely unmelanized except on anterior/dorsal surface between/adjacent to well-developed inverted-Y adfrontal ridges, and on 'mouth frame'/hypostomal ridges extending along, and backwards from, mandibular articulation (Fig. 4k, l); posterior/ventral side closed by a somewhat thickened, but unmelanized and apparently medially complete, cuticular bridge between the hypostomal ridges. Tiny antennae laterally bordered by well-developed strips of cranial cuticle, hence distinctly inside cranial margin (Fig. 4l). Corpotentorium much shorter than in Micropterigidae but still a firm bridge (Fig. 4m); anterior tentorial arms extremely delicate, extending to lateral corpotentorium bases. No labial palp identifiable. Prelabio-hypopharyngeal lobe blunt, with labial gland opening on apex; no discrete distal spinneret process present.

(iii) Pupa. Exarate and denticous. Head (Fig. 4n) on dorsum with large, somewhat raised medial area with prominent rugosity formed by close-set pointed cones; this formation, without counterparts in other homoneurous Lepidoptera, almost certainly plays a role, together with the mandibles, in breaking the bark cover of the cell upon the adult's emergence. Mandibles well-developed and strongly sclerotized, but not hypertrophied and angularly bent; labrum setose, but no demarcated and setose anteclypeus identifiable.

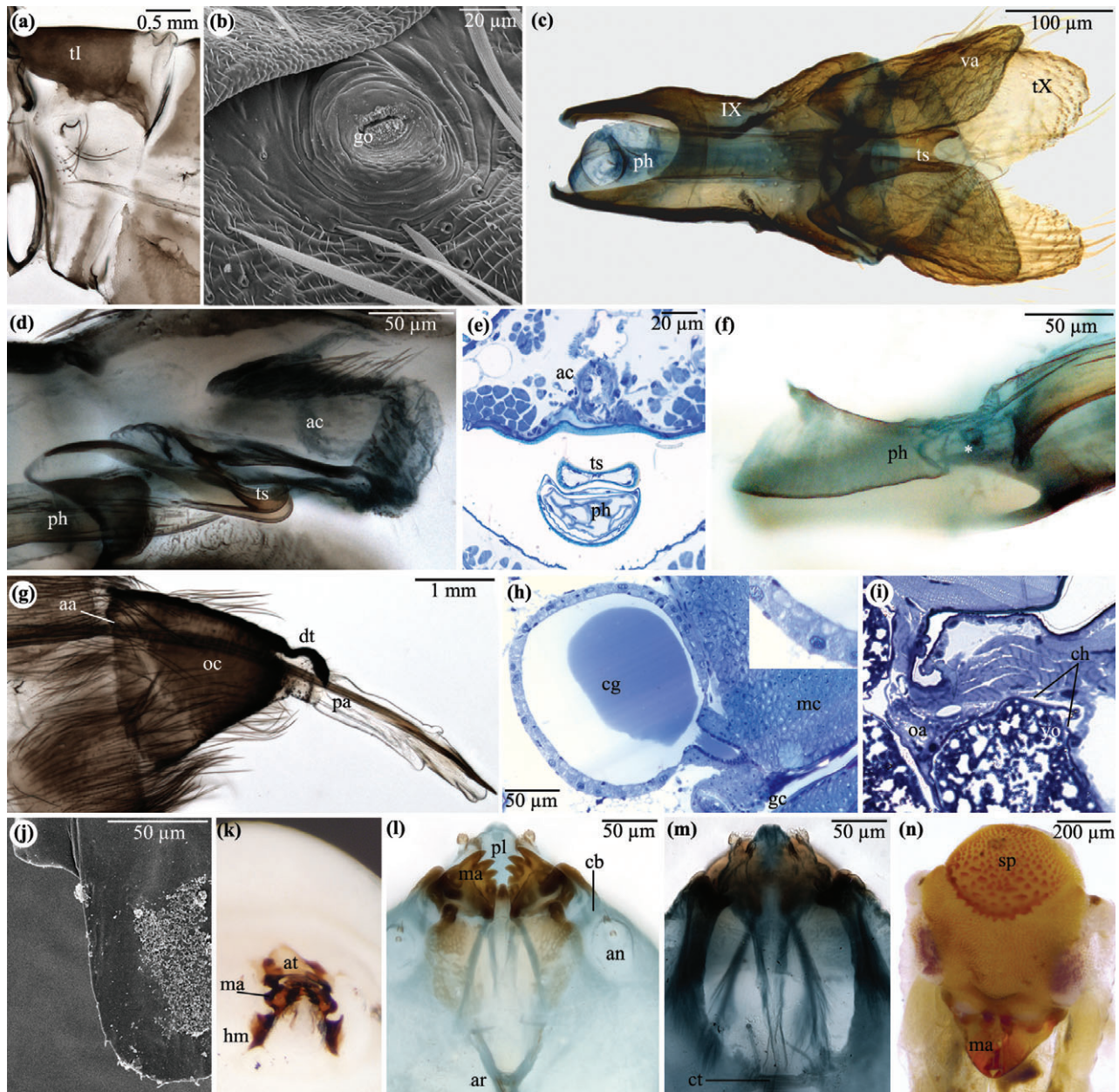


Fig. 4. *Aenigmatinea glatzella*, structure of pregenital abdomen, genitalia, and heads of immatures. (a) Thoraco-abdominal boundary area, coxa and unsclerotized metepimeron removed; (b) papilla of sternum V gland behind IV–V intersegmental fold; (c–f) structures of male genital segments: (c) entire apparatus, ventral view; (d) anal cone and posterior periphallal region, paramedian inner view (left body wall removed by microtome sectioning); (e) same region, transverse section of fixed specimen; (f) anterior part of phallus, same preparation as in (d) – note the soft-walled/flexible zone (asterisk); (g) female postabdomen with extended oviscapt, lateral view; (h) female genital chamber, near-median sagittal section close to opening of colleterial gland; inset: 'type 1' gland epithelium at higher magnification; (i) anterior end of ovariole (at dorsal meso-prothoracic boundary, anterior to right); (j) apex of oviscapt, dorsal view; (k) head of fixed intact larva; (l–m) slide-mounted larval head in anterior/dorsal (l) and posterior/ventral (m) view; (n) pupal head (as seen in pharate adult), anterior view. aa, origin site of anterior apophysis; ac, anal cone; an, antenna; ar, adfrontal ridge(s); at, adfrontal triangle; cb, cranial bridge between antennal base and mandibular articulation; cg, colleterial gland (with contents); ch, chorion; ct, corpotentorium; dt, 'dorso-terminal lobe' of oviscapt cone; gc, genital chamber; go, gland opening; hm, hypostomal margin; ma, mandible; mc, muscular coat (originating on oviscapt cone wall) of genital chamber; oa, ovariole apex; oc, oviscapt cone; pa, posterior apophysis; ph, phallus; pl, prelabio-hypopharyngeal lobe; sp, spinose plate; ts, 'transtilla'; tl, tergum I; tX, lobe of tergum X; va, valve; yo, yolk; IX, segment IX (complete sclerotized ring with deep anteromedian concavity).

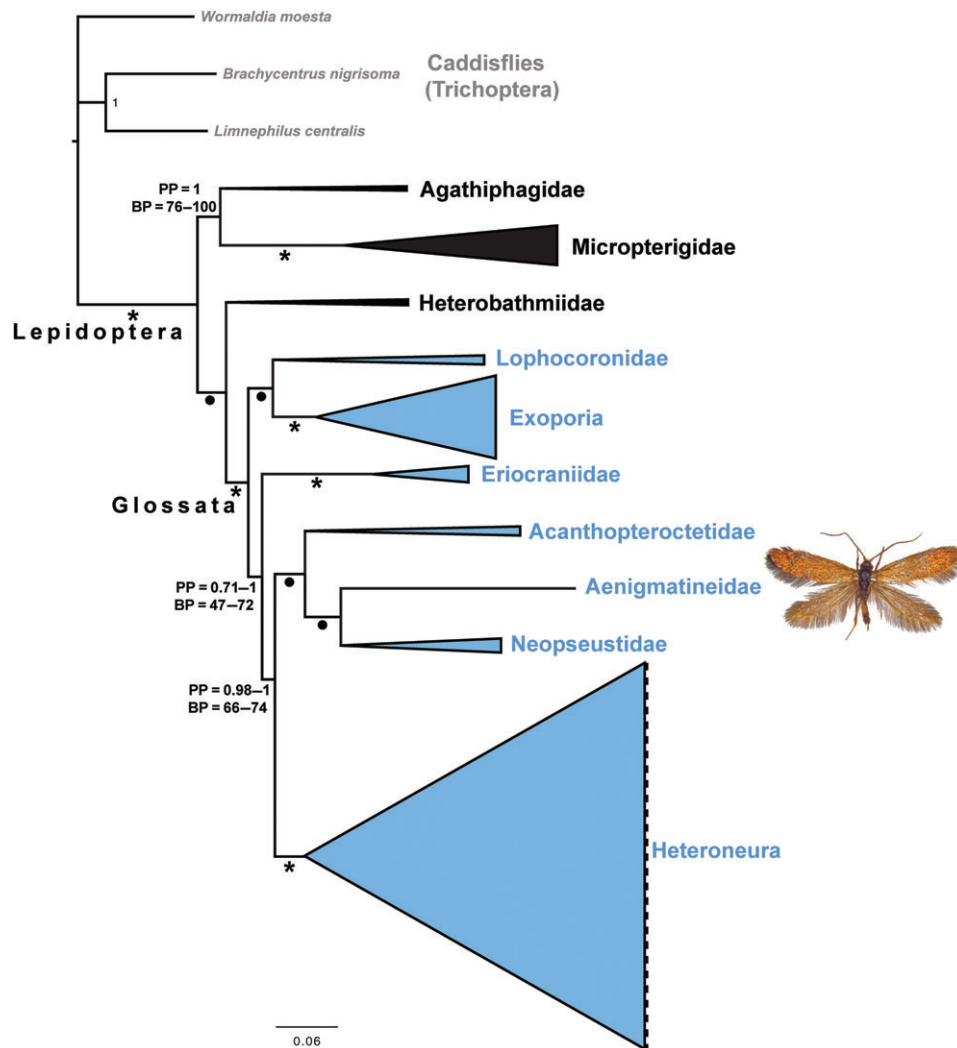


Fig. 5. Cladogram of basal (non-ditrysian and lowest-grade ditrysian) Lepidoptera. Trichopteran outgroups shown in grey. Branch support is as follows: *, posterior probability (PP) = 1, maximum likelihood bootstrap (ML BP) = 100; •, PP = 0.99–1, ML BP = 90–99; or as shown on branches themselves. ‘Jaw moths’ shown in black, and ‘tongue moths’ in blue. Width of terminal triangles approximates the number of described species (van Nieukerken *et al.*, 2011) in each lineage: Micropterigidae (160 spp.), Agathiphagidae (two spp.), Heterobathmiidae (three spp.), Lophocoronidae (six spp.), Exoporia (636 spp.), Eriocraniidae (29 spp.), Acanthopteroctetidae (five spp.), Aenigmatineidae (one sp.), Neopseustidae (14 spp.), and Heteroneura (156 568 spp.).

Molecular analysis

The tree shown in Fig. 5 is the result of the analysis of the dataset (full_ex78) from which the fastest-evolving sites were excluded using the program TIGER (Cummins & McInerney, 2011), partitioned using a previously described procedure (Rota & Wahlberg, 2012), and analyzed with MRBAYES v.3.2 (Ronquist *et al.*, 2012). The topology is identical to that recently presented in Regier *et al.* (2013), except that in the latter, the Eriocraniidae appear as sister group to all other Glossata. It is particularly noteworthy that the Acanthopteroctetidae + Neopseustidae clade, weakly supported in previous molecular studies (Mutanen *et al.*, 2010; Regier *et al.*, 2013) becomes strongly supported when *Aenigmatinea* is included in the analysis. It now comes

to include that taxon as well, as sister group to Neopseustidae, also with strong support.

Discussion

While the mouthparts of adult *Aenigmatinea* are so reduced that they permit no decision on whether or not the moth pertains to the non-glossatan grade, evidence from other anatomical traits (absence of free tritocerebral commissure, thickened cuticular ocellus lens, structure of first thoracic spiracle, mesobasisternal contour, perforations in wing scales), as well as the molecular analysis, convincingly places it as subordinate in the Glossata. Hence its minute galeae are with certainty a reduced tongue,

not a tongue forerunner. The few apparent pre-glossatan-grade character states in *Aenigmatinea* must, then, be considered reversals. They include the ‘type 1’ (Noirot & Quennedey, 1974) rather than ‘type 3’ female colleterial gland cells (shared with all non-glossatans, Hünefeld & Kristensen, 2012), the larva’s rigid and rather stout corpulentorium (shared only with micropterigids, where it is considerably larger, however) and its lack of an articulated spinneret; the reduction of the latter is consistent with the apparent, and quite unusual, absence of any role of silk-spinning in any phase of larval life.

Arguably the principal phylogenetic significance of the discovery of *Aenigmatinea* is that its inclusion in the molecular analysis results in strong support for the Acanthopteroctetidae + Neopseustidae clade, within which it is now placed. This clade was one of the major changes relative to the previous ‘near consensus’ phylogeny retrieved in the recent large-scale analyses (Mutanen *et al.*, 2010; Regier *et al.*, 2013), but being then only weakly supported, and not appearing particularly plausible from a morphological perspective it has so far not attracted much attention. Sets of specializations shared pairwise between the three member lineages of the Acanthopteroctetidae + Aenigmatineidae + Neopseustidae assemblage (henceforth AAeN) are identifiable: *Aenigmatinea* and neopseustids share a strong precoxal bridge between the prothoracic pleuron and sternum, which is also ascribed to the heteroneuran ground pattern (Nielsen & Kristensen, 1996). *Aenigmatinea* and acanthopteroctetids share in their male genitalia the remarkably similarly shaped ‘transtilla’, otherwise unrecorded in the homoneurous grade. They also share the absence of posteromedial arms on the cervical sclerites, otherwise ascribed to the lepidopteran ground pattern and occurring throughout the homoneurans. Acanthopteroctetids and neopseustids share specializations in their antennal structure, i.e. the distinct peg-and-socket articulation of scape and pedicel, the smooth scapopedicellar intercalary sclerite, flagellar hair-like scales that are largely longitudinally aligned and with contiguous sockets (Kristensen *et al.*, 2014). Given the strong molecular support for AAeN monophyly reported here, the lack of clear morphological evidence for the clade as a whole is surprising. A possible homology of the acanthopteroctetid/aenigmatineid ‘transtilla’ with the neopseustid ‘gnathos’ deserves scrutiny, but a definitive elucidation of this issue is probably dependent on availability of additional material of the very rare *Archeptolus schmidi* Mutuura, 1971, which is an overall generalized member of Neopseustidae, and in which a valve–gnathos continuity seems particularly likely from published illustrations (Mutuura, 1971; Davis, 1975). Ascribing any of the other aforementioned apomorphy sets to the AAeN ground pattern evidently necessitates postulating loss in one of its three constituent lineages.

The previous ‘near-consensus’ phylogeny included a clade ‘Myoglossata’ (= Neopseustidae + Exoporia + Heteroneura) characterized primarily by the coilable tongue having an intrinsic musculature, enabling tight coiling in repose (Krenn, 2010). The recently indicated (Regier *et al.*, 2013), and in the present analysis strongly supported, clade comprising Lophocoronidae (without intrinsic tongue muscles) + Exoporia

(with such muscles present in members with fully developed tongue) contradicts myoglossatan monophyly and suggests that this musculature must have independently evolved in Exoporia and elsewhere. A consequence of the strong support for AAeN monophyly here established is additional homoplasy in tongue musculature evolution, which either occurred independently in Neopseustidae and Heteroneura, or in the AAeN + Heteroneura stem lineage with subsequent loss in Acanthopteroctetidae and *Aenigmatinea*. Similarly, the sharply upturned anterior part of the first abdominal tergum, providing a sizeable near-vertical insertion area for the metathoracic indirect wing depressors, previously considered another diagnostic specialization of Myoglossata (Nielsen & Kristensen, 1996), is lacking in acanthopteroctetids and *Aenigmatinea*. Hence, either it is a parallelism not only in exoporians and Neopseustidae + Heteroneura, but also in the two last-mentioned, or it is a parallelism in exoporians and the AAeN + Heteroneura stem lineage with independent losses in Acanthopteroctetidae and *Aenigmatinea*. The prominent anterior mesobasisternal process articulating with spinasternum 1 is a specialization present in neopseustids as well as Heteroneura (Nielsen & Kristensen, 1996), but must have evolved independently in the two, as its absence in *Aenigmatinea* and acanthopteroctetids contradicts ascribing it to the AAeN ground pattern. Labral retractor muscles were previously believed to have been lost just once in adult Lepidoptera (in the stem lineage of all Glossata except eriocraniids and acanthopteroctetids), but now three independent losses must be postulated: in Lophocoronidae + Exoporia, in *Aenigmatinea* + Neopseustidae, and in Heteroneura.

Altogether, then, the discovery of *Aenigmatinea* not only lends additional support to the challenges of the previous ‘near-consensus’ phylogeny of basal lepidopterans from the recent molecular analyses (Mutanen *et al.*, 2010; Regier *et al.*, 2013), but also reveals that early Lepidoptera evolution was even more complex than implied in these studies, in as much as it requires a considerable number of additional ad hoc assumptions of homoplasy to be made.

The presence of an ‘Eriocrania-type’ oviscapt in *Aenigmatinea*, which also occurs in Eriocraniidae, Acanthopteroctetidae and Lophocoronidae (Nielsen & Kristensen, 1996), with dorsal and ventral sclerotizations of segment VIII fused to form an ‘oviscapt cone’, concealing in repose a sclerotized terminal ‘oviscapt saw’ with long, anteriorly projecting, rod-like apodemes serving attachments of muscles which can cause considerable extension, lend strong support to the counterintuitive ascription of this specialized type to the glossatan ground pattern (Nielsen & Kristensen, 1996); hence the derivation of all other glossatan configurations therefrom. Details are considerably different, however. Thus the near-transverse and dorsal muscle mass from the segment VIII cone to the genital chamber in *Aenigmatinea* is very different from the near-longitudinal and ventral cone muscles in Eriocraniidae (conditions in lophocoronids and acanthopteroctetids remain unknown), and *Aenigmatinea* has no counterparts of the ‘ventral rods’ found in the other families.

While angiosperm-independent lifestyles in the pre-glossatan families Micropterigidae (largely bryophyte,

fungus/detritus-feeders) and Agathiphagidae (conifer seed miners) may represent ancestral states, members of the stem-lineage of Heterobathmiidae + Glossata probably switched to angiosperm feeding, as evidenced by this strategy in Heterobathmiidae, Eriocraniidae and Acanthopteroctetidae. Lophocoronid and neopseustid larvae and their habits remain unknown, but it is currently most parsimonious to assume the conifer association of *Aenigmatinea* to be secondary.

Supporting Information

Additional Supporting Information may be found in the online version of this article under the DOI reference: 10.1111/syen.12115

Figure S1. *Aenigmatinea glatzella* sp.n. (a, b) male genital segments in dorsal (a) and lateral (b) view; (c) field photograph of female ovipositing in apex of *Callitris* foliage; (d) ductus spermathecae, transverse section; (e) female postabdomen with extended oviscapt, surface structure in lateral view. ac, collar-like body wall uniting (anus bearing) abdominal tip with preceding part of oviscapt; an, anal cone; oc, oviscapt cone; ph, phallus; tc, thick-walled compartment; ts, ‘transtilla’; tX, lobe of tergum X; IX, segment IX.

Table S1. List of sampled taxa, loci, and their GenBank accession numbers.

Table S2. The number of base pairs analysed for each taxon and locus.

Table S3. List of the eight different data sets analysed (see text for details).

Appendix S1. Supplementary descriptive details.

Acknowledgements

We thank Bushland Conservation Pty Ltd for permission to access their property, which contains most of the current known range of this species; J. Naumann and D. Cheung for technical help with sectioning and illustrations. M. Horak facilitated the 2012 fieldwork. We thank Don Davis, Erik van Nieuwerkerken, and Thomas Simonsen for comments on the manuscript. N.P.K. had economic support from B. Benzons Støttefond. DNA sequencing was supported by an honorarium from the Hermon Slade Foundation to D.J.H.; J.R. and N.W. thank Kone Foundation for funding. The authors declare no conflicts of interest.

References

- ABRS (1998) *Flora of Australia, Volume 48: Ferns, Gymnosperms and Allied Groups*. Australian Biological Resources Study & CSIRO Publishing, Canberra.
- Ax, P. (2000) *The Phylogenetic System of the Metazoa*. Springer-Verlag, Berlin, Heidelberg, New York, New York.

- Brown, J.M., Hedtke, S.M., Lemmon, A.R. & Lemmon, E.M. (2010) When trees grow too long: investigating the causes of highly inaccurate Bayesian branch-length estimates. *Systematic Biology*, **59**, 145–161.
- Cummins, C.A. & McInerney, J.O. (2011) A method for inferring the rate of evolution of homologous characters that can potentially improve phylogenetic inference, resolve deep divergence and correct systematic biases. *Systematic Biology*, **60**, 833–844.
- Davies, M., Twidale, C.R. & Tyler, M.J. (eds) (2002) *Natural History of Kangaroo Island*, 2nd edn. Royal Society of South Australia, Adelaide.
- Davis, D.R. (1975) Systematics and zoogeography of the family Neopseustidae with a proposal of a new superfamily (Lepidoptera: Neopseustoidea). *Smithsonian Contributions to Zoology*, **210**, 1–44.
- Grabherr, M.G., Haas, B.J., Yassour, M. *et al.* (2011) Full-length transcriptome assembly from RNA-Seq data without a reference genome. *Nature Biotechnology*, **29**, 644–U130.
- Grimaldi, D. & Engel, M.S. (2005) *Evolution of the Insects*. Cambridge University Press, New York, New York.
- Hennig, W. (1966) *Phylogenetic Systematics*. University of Illinois Press, Urbana, Illinois.
- Hünefeld, F. & Kristensen, N.P. (2012) The female postabdomen and genitalia of the basal moth family Heterobathmiidae (Insecta: Lepidoptera): structure and phylogenetic significance. *Arthropod Structure & Development*, **41**, 395–407.
- Krenn, H.W. (2010) Feeding mechanisms of adult Lepidoptera: structure, function, and evolution of the mouthparts. *Annual Review of Entomology*, **55**, 307–327.
- Kristensen, N.P., Scoble, M.J. & Karsholt, O. (2007) Lepidoptera phylogeny and systematics: the state of inventorying moth and butterfly diversity. *Zootaxa*, **1668**, 699–747.
- Kristensen, N.P., Rota, J. & Fischer, S. (2014) Notable plesiomorphies and notable specializations: head structure of the primitive “tongue moth” *Acanthopteroctetes unifascia* (Lepidoptera: Acanthopteroctetidae). *Journal of Morphology*, **275**, 153–172.
- Langmead, B. & Salzberg, S.L. (2012) Fast gapped-read alignment with Bowtie 2. *Nature Methods*, **9**, 357–359.
- Li, H. & Durbin, R. (2009) Fast and accurate short read alignment with Burrows–Wheeler transform. *Bioinformatics*, **25**, 1754–1760.
- Linné, C. (1767) *Systema naturæ, Tom. I. Pars II. Editio duodecima reformata*. Salvius, Holmiæ.
- Liu, Y.C., Schroder, J. & Schmidt, B. (2013) Musket: a multistage k-mer spectrum-based error corrector for Illumina sequence data. *Bioinformatics*, **29**, 308–315.
- Marshall, D.C. (2010) Cryptic failure of partitioned Bayesian phylogenetic analyses: lost in the land of long trees. *Systematic Biology*, **59**, 108–117.
- Miller, M.A., Pfeiffer, W. & Schwartz, T. (2010) Creating the CIPRES Science Gateway for inference of large phylogenetic trees. *Proceedings of the Gateway Computing Environments Workshop (GCE)*. New Orleans, Louisiana, 14 November 2010, pp. 1–8.
- Mutanen, M., Wahlberg, N. & Kaila, L. (2010) Comprehensive gene and taxon coverage elucidates radiation patterns in moths and butterflies. *Proceedings of the Royal Society of London, Series B: Biological Sciences*, **277**, 2839–2848.
- Mutuura, A. (1971) A new genus of a homoneurous moth and the description of a new species (Lepidoptera: Neopseustidae). *Canadian Entomologist*, **103**, 1129–1136.
- Nielsen, E.S. & Kristensen, N.P. (1996) The Australian moth family Lophocoronidae and the basal phylogeny of the Lepidoptera-Glossata. *Invertebrate Taxonomy*, **10**, 1199–1302.
- van Nieuwerkerken, E.J., Kaila, L., Kitching, I.J. *et al.* (2011) Order Lepidoptera. *Animal Biodiversity: An Outline of Higher-level*

- Classification and Survey of Taxonomic Richness* (ed. by Z.-Q. Zhang). *Zootaxa*, **3148**, 212–221.
- Noirot, C. & Quennedey, A. (1974) Fine structure of insect epidermal glands. *Annual Review of Entomology*, **19**, 61–80.
- Peña, C. & Malm, T. (2012) VoSeq: a voucher and DNA sequence web application. *PLoS ONE*, **7**, e39071.
- Pye, M.G., Gadek, P.A. & Edwards, K.J. (2003) Divergence, diversity and species of the Australasian *Callitris* (Cupressaceae) and allied genera: evidence from ITS sequence data. *Australian Systematic Botany*, **16**, 505–514.
- Rambaut, A. & Drummond, A.J. (2007) *Tracer v1.4* [WWW document]. URL <http://beast.bio.ed.ac.uk/Tracer> [accessed on 10 May 2010].
- Regier, J.C., Mitter, C., Zwick, A. *et al.* (2013) A large-scale, higher-level, molecular phylogenetic study of the insect order Lepidoptera (moths and butterflies). *PLoS ONE*, **8**, e58568.
- Ren, F., Tanaka, H. & Yang, Z. (2005) An empirical examination of the utility of codon-substitution models in phylogeny reconstruction. *Systematic Biology*, **54**, 808–818.
- Ronquist, F., Teslenko, M., van der Mark, P. *et al.* (2012) MrBayes 3.2: efficient bayesian phylogenetic inference and model choice across a large model space. *Systematic Biology*, **61**, 539–542.
- Rota, J. & Wahlberg, N. (2012) Exploration of data partitioning in an eight-gene data set: phylogeny of metalmark moths (Lepidoptera, Choreutidae). *Zoologica Scripta*, **41**, 536–546.
- Rota-Stabelli, O., Lartillot, N., Philippe, H. & Pisani, D. (2013) Serine codon-usage bias in deep phylogenomics: pancrustacean relationships as a case study. *Systematic Biology*, **62**, 121–133.
- Schulz, M.H., Zerbino, D.R., Vingron, M. & Birney, E. (2012) Oases: robust de novo RNA-seq assembly across the dynamic range of expression levels. *Bioinformatics*, **28**, 1086–1092.
- Stamatakis, A., Hoover, P. & Rougemont, J. (2008) A rapid bootstrap algorithm for the RAxML web-servers. *Systematic Biology*, **75**, 758–771.
- Thorvaldsdottir, H., Robinson, J.T. & Mesirov, J.P. (2013) Integrative Genomics Viewer (IGV): high-performance genomics data visualization and exploration. *Briefings in Bioinformatics*, **14**, 178–192.
- Upton, M.S. & Mantle, B. (2010) *Methods for Collecting, Preserving and Studying Insects and Other Terrestrial Arthropods*. Australian Entomological Society, Canberra.
- Wahlberg, N. & Wheat, C.W. (2008) Genomic outposts serve the phylogenomic pioneers: designing novel nuclear markers for genomic DNA extractions of Lepidoptera. *Systematic Biology*, **57**, 231–242.
- Zerbino, D.R. & Birney, E. (2008) Velvet: algorithms for de novo short read assembly using de Bruijn graphs. *Genome Research*, **18**, 821–829.

Accepted 17 October 2014